Nephrol Dial Transplant (2005) 20: 2783–2792
doi:10.1093/ndt/gfi138
Advance Access publication 4 October 2005

Original Article

Nephrology Dialysis Transplantation

Beneficial effects of aminoguanidine on peritoneal microcirculation and tissue remodelling in a rat model of PD

Mohammad Zareie[1], Geert-Jan Tangelder[2], Piet M. ter Wee[3], Liesbeth HP Hekking[1], Anton A. van Lambalgen[2], Eelco D. Keuning[1], Inge L. Schadee-Eestermans[1], Casper G. Schalkwijk[4], Robert HJ Beelen[1] and Jacob van den Born[1]

[1]Departments of Molecular Cell Biology and Immunology, [2]Department of Physiology, [3]Department of Nephrology and [4]Department of Clinical Chemistry, VU University Medical Center, Amsterdam, The Netherlands

Abstract

Background. The formation of glucose degradation products (GDPs) and accumulation of advanced glycation end products (AGEs) partly contribute to the bioincompatibility of peritoneal dialysis fluids (PDF). Aminoguanidine (AG) scavenges GDPs and prevents the formation of AGEs.

Methods. In a peritoneal dialysis (PD) rat model, we evaluated the effects of the addition of AG to the PDF on microcirculation and morphology of the peritoneum, by intravital microscopy and quantitative morphometric analysis.

Results. AG-bicarbonate effectively scavenged different GDPs from PDF. Daily exposure to PDF for 5 weeks resulted in a significant increase in leucocyte rolling in mesenteric venules, which could be reduced for ~50% by addition of AG-bicarbonate ($P < 0.02$). Vascular leakage was found in rats treated with PDF/AG-bicarbonate, but not with PDF alone. Evaluation of visceral and parietal peritoneum showed the induction of angiogenesis and fibrosis after PDF instillation. PDF/AG-bicarbonate significantly reduced vessel density in omentum and parietal peritoneum ($P < 0.04$), but not in mesentery. PDF-induced fibrosis was significantly reduced by AG ($P < 0.02$). PDF instillation led to AGE accumulation in mesentery, which was inhibited by supplementation of AG. Since addition of AG-bicarbonate to PDF raised pH from 5.2 to 8.5, a similar experiment was performed with AG-hydrochloride that did not change the fluid acidity. We could reproduce most of the results obtained with AG-bicarbonate; however, AG-hydrochloride induced no microvascular leakage and had a minor effect on angiogenesis.

Conclusion. The supplementation of either AG reduced a number of PDF-induced alterations in our model, emphasizing the involvement of GDPs and/or AGEs in the PDF-induced peritoneal injury.

Keywords: aminoguanidine; angiogenesis; fibrosis; peritoneal dialysis; rats

Introduction

There is now accumulating evidence for the bioincompatibility of conventional glucose-based peritoneal dialysis fluids (PDF). These fluids contain high glucose concentrations, which can alter the morphology and function of the peritoneal membrane and has shown to be cytotoxic to peritoneal cells [1]. The process of heat sterilization of PDF leads to the formation of glucose degradation products (GDPs), which are thought to contribute to the toxicity of glucose-based PDF [2]. Upon peritoneal exposure, both high glucose concentrations and the presence of GDPs result in the accumulation of advanced glycation end products (AGEs), which promote angiogenesis, fibrosis and impair host defense mechanisms [3]. In line with these studies, we have previously found various diabetic-like alterations in the peritoneum of rats treated with PDF, including the induction of angiogenesis and fibrosis, which are related to both hyperglycaemia and the presence of GDPs [4,5].

Several lines of evidence suggest aminoguanidine (AG) to be a candidate agent for preventing PDF-induced peritoneal alterations. AG scavenges GDPs [6], prevents the formation of AGEs [6,7] and inactivates inducible NO synthase [8], thereby possessing the ability to reduce the vascular proliferation by modulating the expression of growth factors [3]. In addition, intervention studies with AG in clinical and

Correspondence and offprint requests to: Mohammad Zareie, Department of Molecular Cell Biology and Immunology, VU University Medical Center, PO Box 7057, 1007 MB Amsterdam, The Netherlands. Email: m.zareie@vumc.nl

experimental diabetes have shown the reduction of diabetes-induced pathological changes [7,9]. However, a clinical trial of AG was terminated early for safety concerns. In the PD field, Lamb *et al.* [10] have previously found that the formation of AGEs could be inhibited by AG. Recently, the supplementation of AG to PDF showed inhibitory effects on peritoneal AGE accumulation, mesothelial denudation, submesothelial monocyte infiltration, peritoneal permeability and ultrafiltration [11], and preserved the functional capacity of peritoneal macrophages in the rat [12]. However, the formulation of AG used in most of these studies is not well documented and basic knowledge is lacking on the angiogenic and fibrotic responses as well as on leukocyte–endothelium interactions of the peritoneal membrane after exposing to AG.

In the present study, we evaluated long-term effects of the addition of two different formulations of AG to conventional PDF on quantitative morphometric analysis of the peritoneal membrane, focusing on angiogenesis and fibrosis, as well as on the peritoneal microcirculation by intravital microscopy.

Material and methods

Measurements of glucose degradation products

Glyoxal (GO), methylglyoxal (MGO) and 3-deoxyglucosone (3-DG) were measured by reverse-phase high-performance liquid chromatography, as described before [2].

Animals

Male Wistar rats (Harlan CPB, Horst, The Netherlands) weighing 180–200 g at the beginning of the experiment were used throughout the study. They were allowed to acclimatize 1 week before the experiments started. Animals were maintained under conventional laboratory conditions and were allowed free access to food and water. The experiments were reviewed and approved by the local ethics committee on the use of laboratory animals.

Experimental peritoneal dialysis model

Peritoneal catheters connected to subcutaneous mini-vascular access ports were implanted, as previously described [4,5]. During the first week post-operation all animals, except control animals, received 2 ml of saline with 1 U/ml heparin to allow wound healing. Thereafter, 10 ml of PDF was given daily, for 5 weeks, between 0900 and 1200 hours without the addition of heparin or antibiotics.

Experimental design

Experiment A. Rats were divided into three groups. The first group (PDF, at the start: $n = 10$) received heat-sterilized, lactate-buffered PDF with a pH 5.2 and containing 3.86% glucose (Dianeal® PD4, Baxter Healthcare, Utrecht, The Netherlands), in the second group 1 g/l AG-bicarbonate (Sigma, St. Louis) was added to PDF (AG-bicarbonate, at the start: $n = 11$), and finally untreated rats (control, $n = 7$) served as controls. Thereafter, all animals were subjected to intravital microscopy in order to study the leukocyte–endothelium interactions, such as leukocyte rolling and adhesion, as well as vascular permeability. In addition, the cellular/morphological changes of various peritoneal tissues were studied, including angiogenesis, fibrosis, omental milky spot reaction and mesothelial regeneration response.

Experiment B. Rats received the conventional PDF (Dianeal 3.86%, at the start: $n = 10$) or PDF supplemented with AG-hydrochloride (1 g/l, Sigma, St Louis; at the start: $n = 15$). Untreated rats served as controls ($n = 7$). In this experiment, vascular permeability of the mesenteric venules and cellular/morphological alterations of peritoneal tissues were studied.

Intravital microscopy

Experiment A. After 5 weeks of treatment, rats were anaesthetized and cannulated, as described previously [13]. Thereafter, blood samples were collected and cells were differentiated using a Helios cell counter (ABX Diagnostics) implemented with rat-specific software. Intravital microscopic observations of the mesenteric venules were performed as described previously [13]. Briefly, the distal ileum was exteriorized from the peritoneal cavity to allow microscopic observations. The area for analysis was selected in a standardized way, i.e. the most distally situated loop of the ileum. During a stabilization period of 30 min, the whole mesentery was video inspected. Thereafter, observation of the mesenteric microcirculation was performed during a 1–2 h period. In each individual rat, 17–33 venules (101–151 venules per group; total 360 venules in all animals) were analysed.

Venular diameter. The inner diameter was measured with a home-made video image shearing device [13].

Leukocyte rolling. Leucocytes were considered to be rolling if they could be seen moving along the vessel wall, by eye, at a significantly lower rate than the blood flow [13]. The number of rolling leukocytes in the venules was determined from the recorded video images by counting the rolling leukocytes per minute passing a reference point in the microvessel.

Leukocyte adhesion. The number of firmly adherent leukocytes was expressed as the number of leukocytes remaining stationary for 30 s or longer in a 100 µm segment of venule during 1 min [13].

Experiments A and B: *Microvascular permeability*. FITC-BSA, 200 mg/kg body weight, dissolved in 0.5 ml 0.9% NaCl, was infused i.v. during 2–3 min in all rats. The luminescent microvessels were observed and video-documented during a period of 45–60 min. The experimental protocol was ended by superfusion with histamine (10 µg/ml) to determine its ability to induce hyperpermeability in the preparation.

Morphological analysis

Omentum and mesentery. Omental (two sections of approximately 4 cm^2/rat) and mesenteric tissues (the most distally situated loop entirely) were dissected, spread on an

object slide and stained with toluidine blue. Omental tissues were inspected for the presence of bacteria in order to exclude silent peritonitis and no bacteria were found. Since omental milky spots (local aggregates of immune cells) are the major route through which leucocytes migrate into the peritoneal cavity and because their number and size reflect the activated state of the omentum, we determined their number and size by light microscopy, using a scored eyepiece, as previously described [4,5]. The total milky spot surface area was calculated by multiplying both the parameters. Likewise, in 25 random areas, the number of blood vessels in omental and mesenteric tissues were counted and expressed as the number of vessels/cm^2. Furthermore, in 10 randomly selected areas of the omentum and mesentery, mast cells were counted and expressed per mm^2 [5]. Mast cells present in/on omental milky spots were excluded from this analysis. Stretch preparations of mesenteric tissues (the second most diatally situated loop of the ileum) were also stained with the monoclonal antibody 4B5 against glycated proteins [14].

Parietal peritoneum. Cryostat sections of large specimens (two portions of approximately 20 cm^2) of the parietal peritoneum were cut (8 μm) and embedded in a standardized fashion. The thickness of the submesothelial extracellular matrix (ECM) was determined after Van Giesson staining (Merck KGaA, Darmstadt, Germany), as described previously [4,5]. Frozen sections were also used to quantify the number of submesothelial blood vessels, using anti-CD31 (PECAM) as the endothelial marker and expressed as the number of vessels per mm length of the mesothelial layer. Cryostat sections were also used to evaluate the formation of granulation tissue after staining with anti-CD31 and Van Giesson, which was characterized by thickening of the ECM (fibrosis), the formation of numerous blood vessels, and cellular infiltrates including mast cells, as previously described [5].

Liver. Mesothelial liver imprints were dried and stained by May Grünwald Giemsa, as described before [4,5]. The number of cells per 0.1 mm^2 area was counted and the average of 16 areas was calculated for each slide and expressed as cells/mm^2.

Electron microscopy of peritoneal tissues

In order to inspect the integrity of the mesothelial cell layer covering the peritoneal membrane, portions of the dissected omentum, mesentery, diaphragm, liver and parietal peritoneum of at least three animals/group were prepared for electron microscopy according to standard procedures [4,5]. Peritoneal fibrosis was measured based on overview electron micrographs of cross sections of mesenteric tissues. The distance between the two mesothelial cell layers was measured at various places on each micrograph and the mean was calculated for each photo. We analyzed 3 rats per group, 10 or more micrographs per rat [5].

Statistical analysis

Data are expressed as medians with the spread from 25th to 75th percentile (interquartile range) and the range from 10th to 90th percentile. Data were statistically analysed using either the non-parametric Kruskal–Wallis, Mann–Whitney *U*-tests or Fisher's exact test. Because three groups were involved, $P < 0.05/\sqrt{n}$, thus $P < 0.03$ was regarded as significant, according to the Bonferroni correction.

Results

Drop-out

Throughout the first experiment, there was a drop-out of 50 and 45% in the PDF and AG-bicarbonate groups, respectively, due to omental wrapping around the tip of the catheter, which was not different among treated groups (Fisher's exact test; $P = 1.0$). After 5 weeks of fluid instillation, 5 and 6 rats in PDF and AG-bicarbonate, respectively, had remained for analysis. We were able to analyse only six of the seven control rats for intravital microscopy, since no appropriate venules could be selected in one animal. All seven rats were used for morphological analysis.

There was a drop-out of 30 and 27% of the animals in PDF and AG-hydrochloride group, respectively, due to omental wrapping around the tip of the catheter, which was not different between treated groups (Fisher's exact test; $P = 0.26$). After 5 weeks of fluid instillation, 7 and 11 rats in PDF and AG-hydrochloride had remained and all (seven) untreated animals were used for analysis.

Kinetic study on scavenging of GDPs by aminoguanidines

In a time-course study, four different concentrations of AG-bicarbonate and AG-hydrochloride (0.01, 0.1, 1 and 10 g/l) were added to the PDF and the amount of three different GDPs, namely GO, MGO and 3-DG, were measured. Addition of 0.01 g/l of both kinds of AG could not scavenge GDPs from PDF. Supplementation of 0.1 g/l of both AGs for 2–3 days scavenged GO and MG effectively, but had barely any effect on 3-DG concentrations. Moreover, 1 g/l of both AGs scavenged effectively GO, MGO and 3-DG from the PDF, but with different kinetics. AG-bicarbonate scavenged GDPs completely within 2–3 days, whereas AG-hydrochloride did not (Figure 1). A higher concentration (10 g/l) of AG-bicarbonate did not solve in PDF, while this concentration of AG-hydrochloride scavenged GDPs faster than lower concentrations (data not shown). Therefore, to ensure the quenching of GDPs, 1 g/l AG-bicarbonate was added to PDF 2–3 days before fluid injection and 1 g/l AG-hydrochloride was supplemented 5 days before fluid instillation. The supplementation of 1 g/l AG-bicarbonate resulted in an elevated pH value of the PDF (from 5.2 to 8.5), whereas AG-hydrochloride had no effect on pH as it remains at 5.2.

Biological and systemic parameters

During both experiments, the well-being of all animals was monitored daily, but no apparent abnormalities were observed. The development of body weight of all

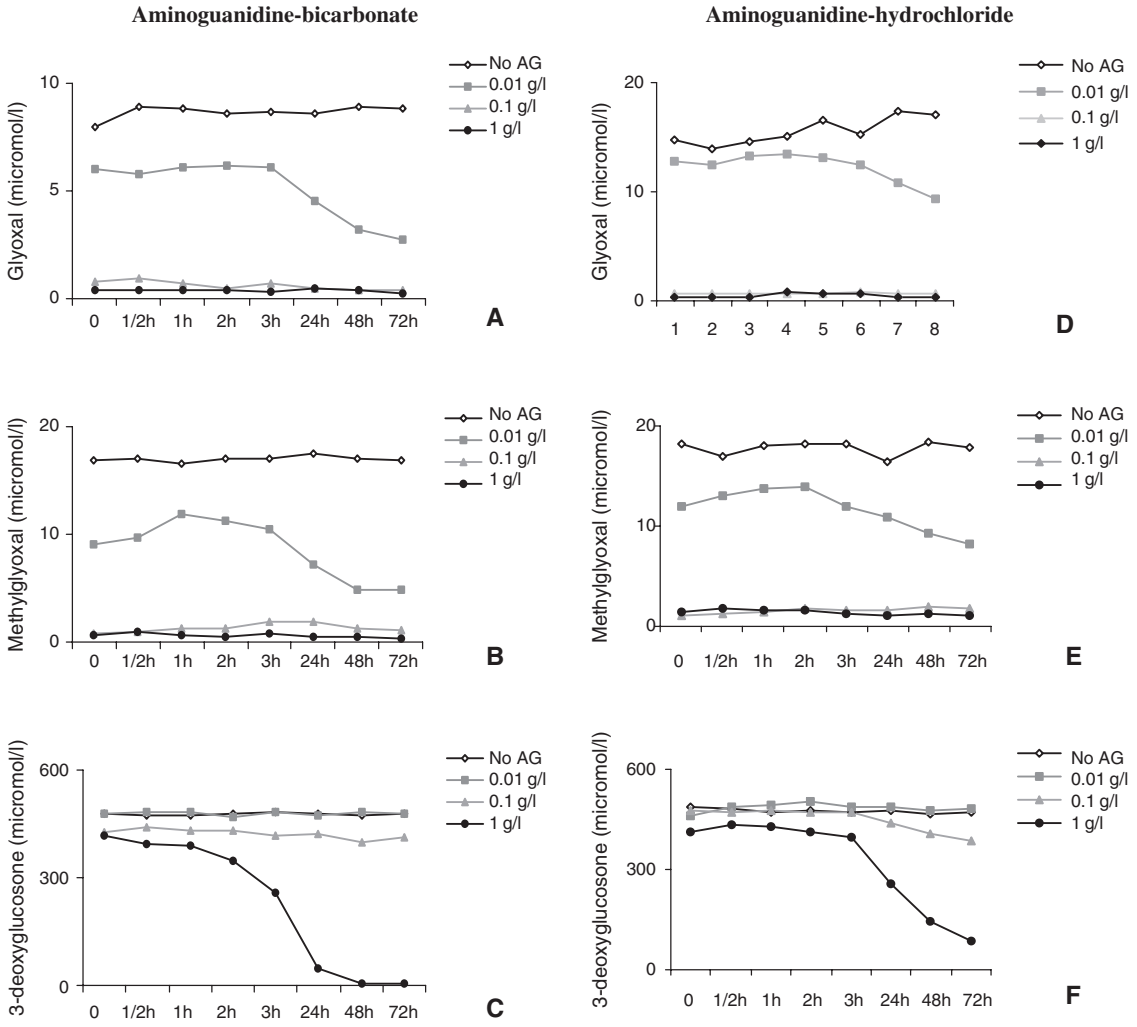

Fig. 1. The time-dependency of the scavenging function of aminoguanidine-bicarbonate (A–C) and aminoguanidine-hydrochloride (D–F) on the concentration of glyoxal (A and D), methylglyoxal (B and E) and 3-deoxyglucosone (C and F) present in the PDF. At time = 0, concentration of different GDPs was measured immediately after dissolving aminoguanidines.

treated animals was normal. In Experiment A, the body weight as well as mean arterial pressure and heart rate did not change significantly in rats exposed to PDF with or without AG-bicarbonate (Table 1). Likewise, no differences were found in the total leukocyte count or in percentages of monocytes, neutrophils, basophils and eosinophils in blood among these groups.

Inflammation-related alterations

Rolling leukocytes were present only in venules, whereas no rolling leukocytes were found in arterioles. Chronic exposure to PDF resulted in approximately 4-fold increase in the number of rolling leukocytes in mesenteric venules compared to control rats (median of 58 *vs* 16 cells/min; $P < 0.008$), irrespective of vessels diameter (Figure 2), which indicates endothelial activation due to PDF exposure. The addition of AG-bicarbonate resulted in a significantly lower number of rolling leukocytes compared to PDF group (median of 32 cells/min; $P < 0.02$). The number of rolling leukocytes was slightly increased in the AG-bicarbonate group compared to the control group, although this difference was not statistically significant ($P = 0.08$). To investigate the distribution

Table 1. Biological and systemic parameters

Experiment A	PDF	AG-bicarbonate	Control
Body weight (g)	394 (390–400)	410 (410–425)	430 (420–440)
Heart rate (beats/min)	354 (354–370)	347 (343–359)	344 (336–357)
Mean arterial pressure (mmHg)	117 (113–135)	113 (100–128)	120 (110–140)
Blood leucocytes			
Number of cells (10^9/l)	9.4 (9.2–11.6)	9.9 (9.1–12.1)	8.7 (7.8–10.3)
% Lymphocytes	60.1 (50.6–67.9)	74.7 (71.6–75.8)	75.3 (66.9–78.7)
% Monocytes	1.9 (1.0–7.1)	3.4 (1.7–4.0)	1.0 (0.80–1.7)
% Neutrophils	27.9 (26.0–32.6)	20.1 (18.6–20.6)	21.8 (20.3–29.2)
% Eosinophils	0.4 (0.4–0.6)	0.3 (0.2–0.3)	0.5 (0.4–0.6)
% Basophils	4.7 (3.6–5.7)	4.0 (3.0–5.1)	3.5 (3.0–4.0)

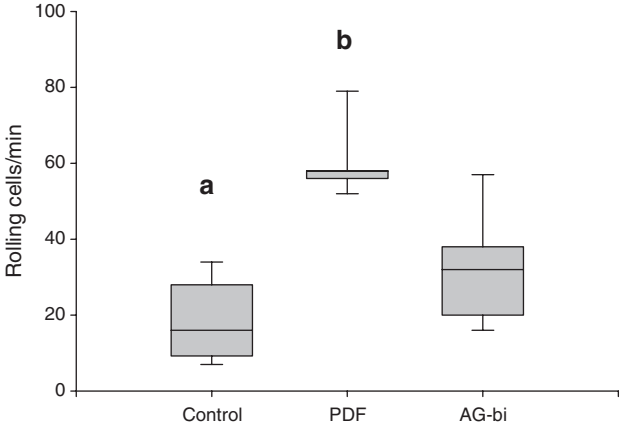

Fig. 2. The number of rolling leucocytes in mesenteric venules (11–40 μm) after 5 weeks exposure to peritoneal dialysis fluid (PDF) with or without aminoguanidine-bicarbonate (AG-bi) and in control rats.
[a]Control *vs* PDF: $P < 0.008$; [b]PDF *vs* AG-bicarbonate: $P < 0.02$.

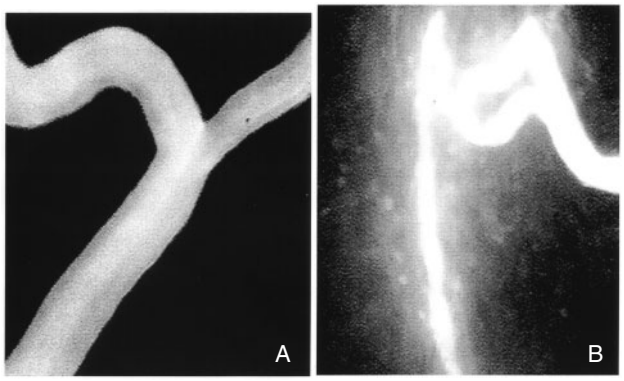

Fig. 3. Rats exposed to PDF showed intact mesenteric vessels after i.v. injection of FITC-labeled albumin (A). In contrast, some of mesenteric vessels from rats exposed to PDF supplemented with aminoguanidine-bicarbonate (AG-bi) in the Experiment A were leaky (B). No vascular leakage was found in controls or rats exposed to PDF supplemented with aminoguanidine-hydrochloride (AG-Hcl) in Experiment B.

of rolling leukocytes within different mesenteric venules, vessels were divided into postcapillary venules (with an inner diameter of 11–25 μm) and collecting venules (with an inner diameter of 26–40 μm). Exposure to PDF resulted in a higher number of rolling leukocytes in both post-capillary and collecting venules, compared to control rats, which was significantly reduced after addition of AG-bicarbonate. The number of spontaneous adherent leukocytes in mesenteric venules was very low (0–2 cells/100 μm/min) and did not differ among the three groups ($P = 0.68$ and $P = 0.42$ in post capillary and collecting venules, respectively). This indicates that the observed rolling in the PDF groups is not secondary to bacterial infection. In addition, no vascular leakage was observed after injection with FITC-labelled albumin in rats exposed to PDF or controls, within a timeframe of 45–60 min. In contrast, focal vascular permeability for albumin (i.e. the number of leaky spots) was significantly increased in mesenteric vessels of animals treated with AG-bicarbonate ($P < 0.003$, Fisher's exact test, Figure 3). The vascular leakage was seen in a minority of venules (<10%), irrespective of their diameter. To investigate whether the observed vascular leakage in AG-bicarbonate was related to its high pH, FITC-labelled albumin was intravenously injected to rats exposed to AG-hydrochloride (Experiment B) and the integrity of venules were inspected for at least 60 min. No vascular leakage was found in rats exposed to PDF supplemented with AG-hydrochloride, suggesting that the vascular leakage induced by AG-bicarbonate is most likely pH-related. Superfusion of histamine resulted in a clear vascular leakage of FITC-labelled albumin within minutes (data not shown).

The histological observation of omentum showed that a daily instillation of conventional PDF for 5 weeks resulted in a strong milky spot response in the omentum, reflecting an activated status of the peritoneum. Both the numbers and the size of milky spots were significantly increased compared to control rats (Table 2). Supplementation of AG-bicarbonate did not significantly affect the PDF-induced milky spot response in the omentum. The addition of AG-hydrochloride had no effect on high number of milky spots induced by PDF; however, the observed spots were smaller than in PDF-treated animals.

Tissue remodelling

Angiogenesis. Daily exposure of the conventional PDF resulted in angiogenesis in the omentum, mesentery and parietal peritoneum (Figure 4). Supplementation of AG-bicarbonate strongly reduced the number of blood vessels in the omentum ($P = 0.03$) and in the parietal peritoneum ($P < 0.03$). The latter, however, was not found with the hydrochloride formulation of AG. Thus, equal number of blood vessels was found in the omentum and parietal peritoneum after exposure to PDF with or without AG-hydrochloride. This suggests that most likely the anti-angiogenic effect of AG is ineffective under low pH conditions. Furthermore, the addition of both types of AG did not significantly change the angiogenic response in the mesentery evoked by PDF, consequently more blood vessels were found in rats treated with either formulation of AG, compared to control rats. These data suggest that the mesentery responds differently from the omentum and parietal peritoneum to PDF exposure.

Fibrosis. In order to quantify peritoneal fibrosis, the width of the ECM of mesenteric tissues was measured at overview electron photomicrographs [5]. Chronic treatment with PDF resulted in a significant thickening of the mesenteric ECM, compared to control rats (Figure 5A and B). This increase in thickness is not due to oedema formation, since we observed a marked increase of collagen bundles without spacing between the bundles [5]. The addition of AG-bicarbonate reduced the PDF-induced fibrosis by ~30%, although

Table 2. Cellular alterations of omentum

	PDF	AG-bicarbonate	Control
AG-bicarbonate			
No. of milky spots/cm^2	25.0 (24.0–25.0)[a]	16.1 (10.9–17.8)[b]	2.5 (1.6–7.5)
Area/milky spots (mm^2)	0.2 (0.2–0.3)[a]	0.3 (0.3–0.3)[b]	0.1 (0.1–0.1)
% Milky spots surface	5.0 (4.3–8.0)[a]	5.4 (2.6–6.5)[b]	0.27 (0.2–1.0)
AG-hydrochloride	PDF	AG-hydrochloride	Control
No. of milky spots/cm^2	31.0 (30.0–47.0)[a]	24.0 (19.1–31.5)[d]	8.9 (5.9–16.7)
Area/milky spots (mm^2)	0.5 (0.5–0.6)[a,c]	0.4 (0.4–0.4)[d]	0.2 (0.1–0.2)
% Milky spots surface	18.2 (16.1–28.4)[a,c]	10.1 (6.7–12.8)[d]	1.4 (0.9–3.1)

[a]PDF *vs* Control: $P < 0.004$; [b]AG-bicarbonate *vs* Control: $P < 0.02$; [c]PDF *vs* AG-hydrochloride: $P < 0.02$; [d]AG-hydrochloride *vs* Control: $P < 0.005$.

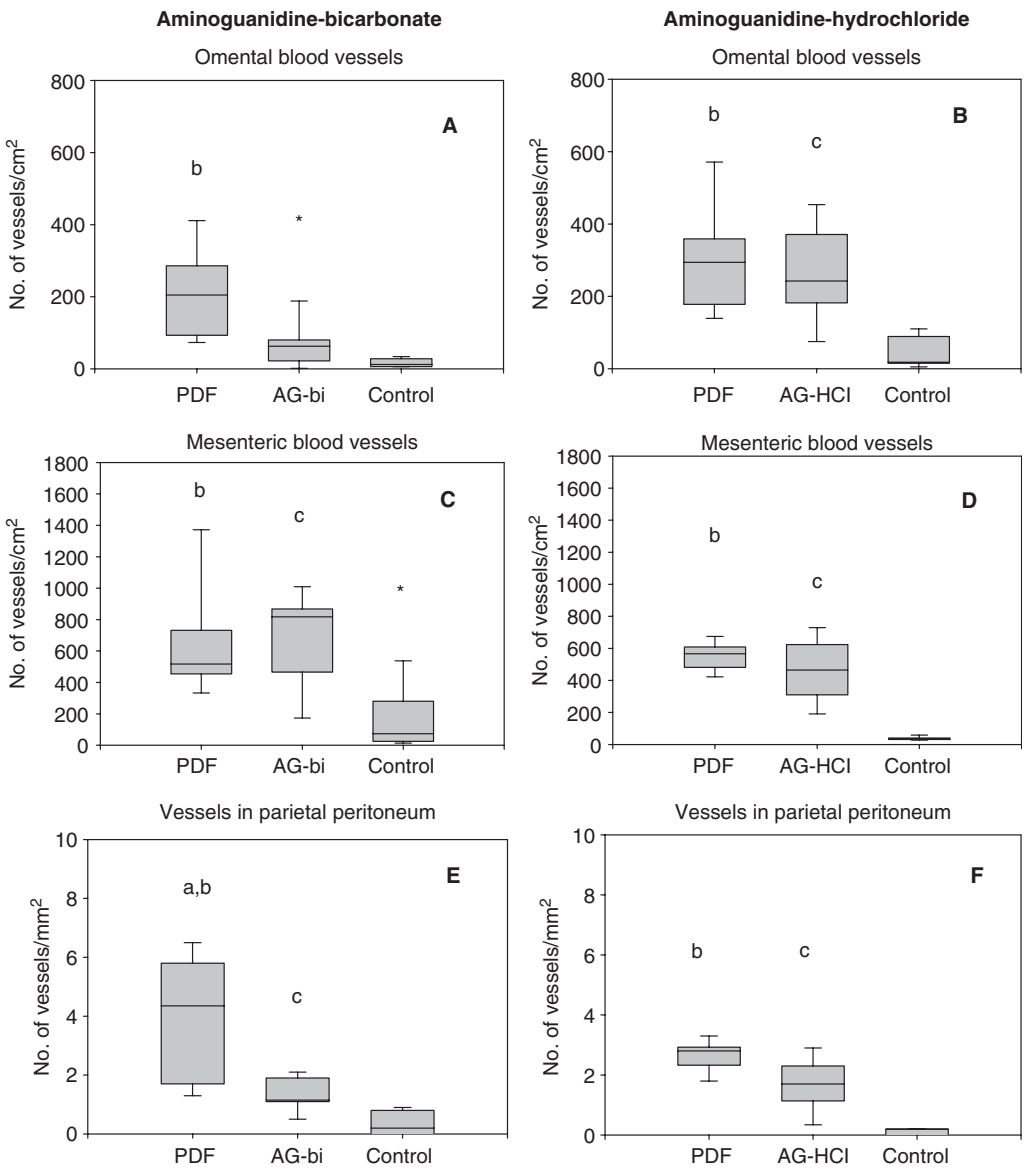

Fig. 4. The number of blood vessels in the omentum (A and B), mesentery (C and D) and the parietal peritoneum (E and F) of rats exposed to peritoneal dialysis fluid (PDF) with or without either aminoguanidine-bicarbonate (AG-bi; A, C and E) or aminoguanidine-hydrochloride (AG-HCl; B, D and F).
[a]PDF *vs* AG-bi: $P < 0.03$; [b]PDF *vs* Control: $P < 0.005$; [c]AG-bi/AG-HCl *vs* Control: $P < 0.02$; *differs from PDF: $P = 0.03$.

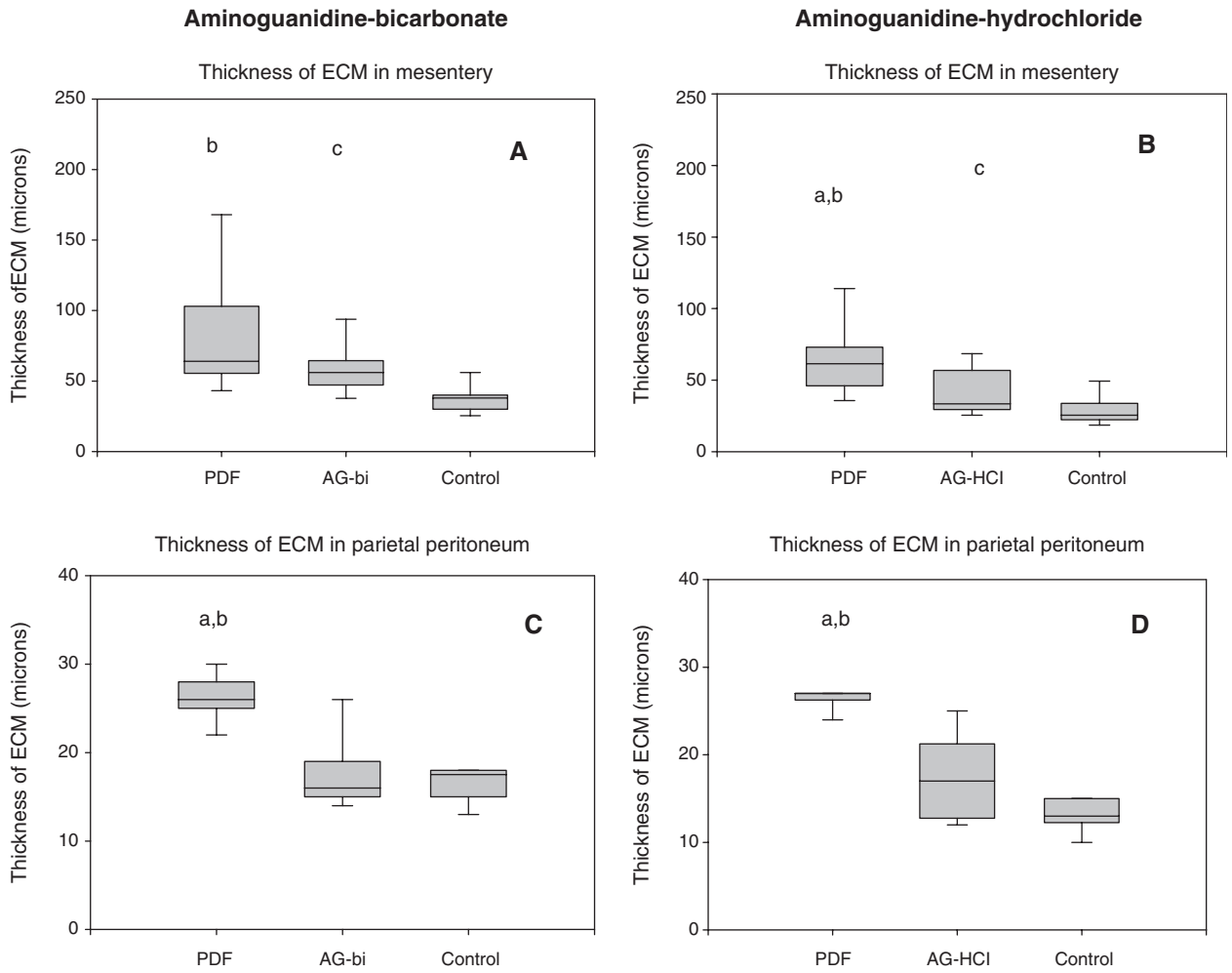

Fig. 5. Fibrosis was quantified by measuring both the width of the submesothelial extracellular matrix (ECM) of the mesentery, based on electron micrographs (A and B) and by measuring the thickness of submesothelial ECM of parietal peritoneum after staining with Van Giesson (C and D) of rats exposed to peritoneal dialysis fluid (PDF) with or without either aminoguanidine-bicarbonate (AG-bi; A and C) or aminoguanidine-hydrochloride (AG-HCl; B and D).
[a]PDF *vs* AG-bi/AG-HCl: $P < 0.02$; [b]PDF *vs* Control: $P < 0.008$; [c]AG-bi/AG-HCl *vs* Control: $P < 0.02$.

not quite significant ($P = 0.09$). Likewise, the supplementation of AG-hydrochloride to PDF largely prevented the PDF-induced increase in mesenteric matrix thickening by ~75% (Figure 5B; $P < 0.005$). However, neither AG-bicarbonate nor AG-hydrochloride could completely prevent the PDF-induced mesenteric fibrosis, as mesenteric tissues were significantly thickened in rats exposed to AG-bicarbonate ($P < 0.0007$) or AG-hydrochloride ($P < 0.02$), compared to control animals.

Frozen sections of parietal peritoneum were also used to address the development of fibrosis [5]. The thickness of the ECM of the parietal peritoneum was significantly increased in rats exposed to PDF (Figure 5C and D). The addition of AG-bicarbonate significantly prevented the fibrosis in the parietal peritoneum ($P < 0.02$), as no significant differences were found between animals treated with PDF supplemented with AG-bicarbonate and control animals ($P = 0.94$). Likewise, the addition of AG-hydrochloride reduced the degree of fibrosis significantly ($P < 0.02$), with no differences between AG-hydrochloride and the control group ($P = 0.31$).

AGE-accumulation. The vascular walls and mesothelial cells in mesenteric tissues from rats exposed to PDF were glycated, as shown by a positive staining with anti-AGE monoclonal antibody 4B5, whereas barely any staining was found in control rats and rats treated with AG-bicarbonate or AG-hydrochloride after staining with monoclonal antibody against AGEs (Figure 6).

Granulation tissue. Large sections of the parietal peritoneum were used to address the development of granulation tissues [5]. All animals treated with conventional PDF developed focal granulation tissues, which, however, were partly prevented by the presence of AG-hydrochloride in the conventional PDF ($P = 0.05$, Fisher's exact test). Only 6 out of 10 rats in the AG-hydrochloride group developed granulation tissues, which were markedly smaller compared to those formed in PDF without AG-hydrochloride.

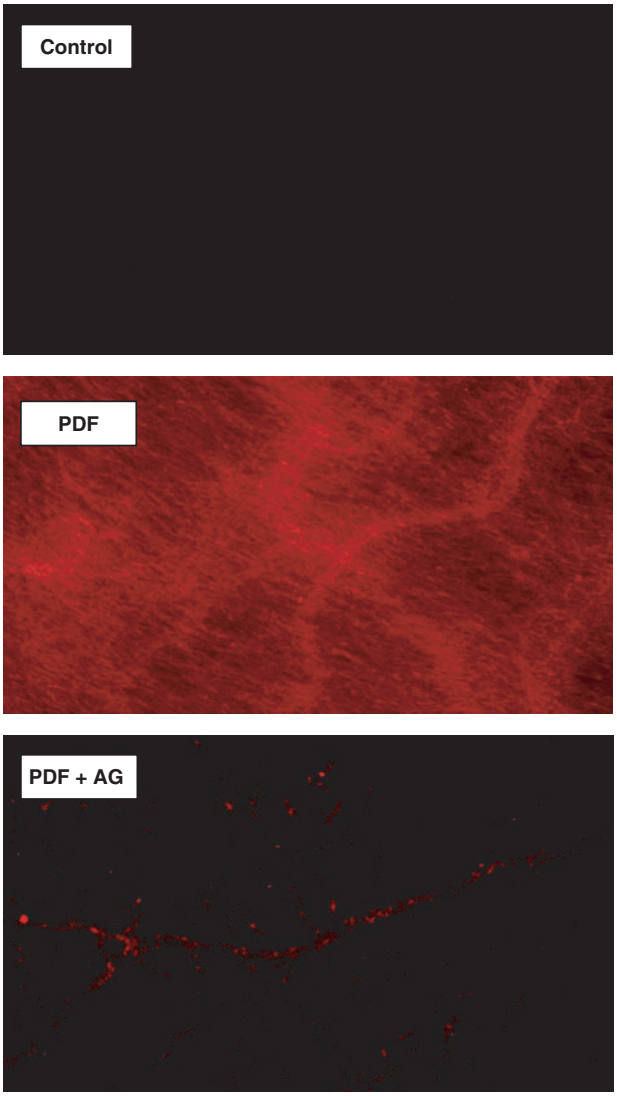

Fig. 6. Representative micrographs of mesenteric tissues of untreated animals (control), and from rats exposed to peritoneal dialysis fluid (PDF) and PDF supplemented with aminoguanidine-bicarbonate (PDF + AG) after staining with anti-AGE antibody, indicating the effective inhibition of AGE formation by aminoguanidine. Addition of aminoguanidine-hydrochloride also prevented the AGE formation (data not shown).

Control rats never showed the presence of granulation tissue. The development of granulation tissues in the AG-bicarbonate group could not be addressed because only small sections of the parietal peritoneum were taken for the analysis.

Mesothelial cells. The density of mesothelial cells on the liver was significantly increased in rats instilled with PDF, compared to control animals (median of 1656 *vs* 1406 cells/mm^2; $P < 0.008$). The addition of either AG to PDF did not influence the PDF-induced regenerative response of the mesothelial cells on the liver, as no significant differences were found between rats exposed to PDF and animals treated with PDF supplemented with AG-bicarbonate ($P > 0.99$) or AG-hydrochloride ($P = 0.52$). Thus, compared to control rats, more mesothelial cells were found in the AG-bicarbonate group, although not quite statistically significant ($P = 0.09$), and in the AG-hydrochloride groups ($P < 0.0002$).

The integrity of the mesothelial cell layers covering different peritoneal tissues (omentum, mesentery, liver, diaphragm and parietal peritoneum) were inspected by electron microscopy (Figure 7). The mesothelial cell layer on the peritoneal surface of both visceral and parietal peritoneum of control animals showed a normal (intact) appearance, thus mesothelial cells and their microvilli were present (Figure 7A). In contrast to control animals, chronic exposure to PDF resulted in a severe damage to the mesothelial cell layer covering the peritoneal membrane, which was characterized by focal loss of microvilli, vacuolization or complete loss of mesothelial cells (Figure 7B). Addition of both kinds of AG did not prevent the PDF-induced mesothelial cell damage (Figure 7C), with no difference between both AGs, and thus, severe damage was found in the AG-bicarbonate and AG-hydrochloride groups. In general, damage to the visceral mesothelial cell layer covering the omentum, mesentery, diaphragm and liver found in all treated groups was profound, whereas, this damage was clearly milder in the parietal peritoneum (data not shown).

Discussion

In the present study, we show that the addition of AG to conventional glucose-containing PDF effectively scavenged GDPs and largely inhibited PDF-induced accumulation of AGEs. Furthermore, AG significantly reduced PDF-induced endothelial activation, angiogenesis and fibrosis. Although two formulations of AG appeared to differ in some aspects, our data clearly demonstrate that AG-derivatives are powerful compounds to reduce PD-related complications and provide novel insights into the pathophysiology of PDF-induced peritoneal injury.

Although the dysfunction of the vascular endothelium is a known risk factor for patients suffering from hyperglycaemia [3], little attention has been paid to the study of the leukocyte–endothelium interactions of the peritoneum during chronic PD. Therefore, we focused on the study of the peritoneal microcirculation, including leukocyte–endothelium interactions as well as vascular permeability, providing useful information regarding the functional status of the endothelium during peritoneal dialysis. We realized that the performance of intravital microscopy did not permit the study of the peritoneal transport parameters in the same animals; however, this has already been studied by others [11]. In the present study, the number of rolling leukocytes in mesenteric venules was approximately 4-fold increased in rats exposed to PDF, which could not be explained by changes in blood flow or systemic leukocyte count [13]. However, a recent study showed a decreased number of rolling leukocytes upon exposure to PDF in rats [15], which might be explained

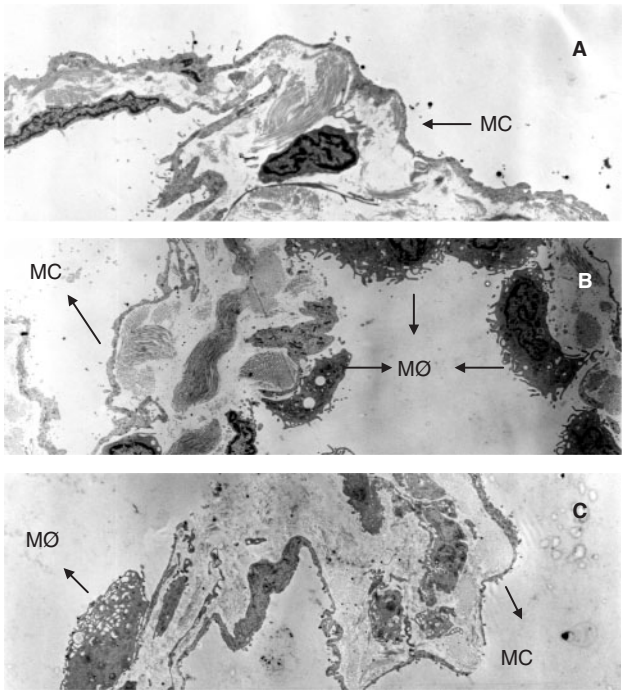

Fig. 7. Representative electron micrographs of omental tissues of control untreated animals (A), and from rats exposed to peritoneal dialysis fluid (PDF) with (C) or without aminoguanidine-hydrochloride (B). The mesothelial cell layer (MC) is intact in control rats, whereas this cell layer is highly damaged in rats exposed to PDF with or without aminoguanidines. No difference was found between both kinds of aminoguanidine. Note that damaged sides (no mesothelial cells) in treated animals were covered by macrophages (Mø).

by a difference in experimental approach, i.e. acute *vs* chronic PDF exposure. Several lines of evidence suggest that chronic exposure to GDPs and/or AGE depositions are involved in the endothelial activation. We and others showed increased levels of soluble endothelial adhesion molecules in continous ambulatory peritoneal dialysis (CAPD) patients [16,17]. We recently showed that exposure of mesothelial cells to reactive aldehydes like MG and 3-DG resulted in cellular uptake of these compounds followed by an inflammatory response of the cells, including an upregulation of the vascular cell adhesion molecule-1 [17], which can potentially be involved in the leukocyte rolling process. The same holds true for AGEs [17]. Thus, we concluded that both neutralization of GDPs and prevention of AGE formation by AG might explain the reduced endothelial activation in this study. In line with this conclusion, our preliminary data revealed less profound leukocyte–endothelium interactions in the mesenteric venules after chronic exposure to a GDP-poor, bicarbonate/lactate-buffered PDF, compared to the conventional PDF containing a high GDP content in our model (data not shown). Furthermore, in our study, the level of adherent leukocytes was not affected by PDF with or without AG, indicating that the elevated level of rolling found in the PDF group was not related to bacterial infection, which is always accompanied by enhanced leukocyte adhesion.

It has been shown that AG strongly reduced fibrosis in the lungs [8]. In agreement with this study, we now show that the addition of AG to PDF completely prevented the PDF-induced peritoneal fibrosis in the parietal peritoneum and largely reduced fibrosis in the mesentery *in vivo*.

Due to the bioincompatible effects of the conventional PDF, more physiological solutions have become available. We [4] and others [18] have already shown that the bicarbonate/lactate buffered, glucose-based PDF (Physioneal) better preserved the function and morphology of the peritoneum in the experimental PD model. The desirable effects of this solution can, partly, be explained by the formation of a lower amount of GDPs. However, the supplementation of AG appears to produce more beneficial effects on the peritoneal morphology and microvasculature than Physioneal. For instance, AG could almost completely inhibit the PDF-induced fibrosis, whereas animals treated with Physioneal developed substantially more fibrosis than control rats [4,18]. Furthermore, our preliminary data revealed more rolling leukocytes in the mesenteric venules after chronic treatment with low GDP content Physioneal compared to rats exposed to the conventional PDF supplemented with AG-bicarbonate (it will be communicated separately). Therefore, we suggest that the beneficial effects of AG on the peritoneal morphology and microcirculation are not only due to its action on GDPs, but also on AGEs [8] and/or NO production.

Besides common beneficial effects of both AG formulations, they also differ from each other in some aspects. First, exposure to PDF supplemented with AG-bicarbonate resulted in a clear albumin leakage in some of the mesenteric venules. No vascular leakage, however, was found in the AG-hydrochloride group. Second, the supplementation of AG-bicarbonate significantly reduced the PDF-induced angiogenesis in both the omentum and in the parietal peritoneum. In contrast, AG-hydrochloride had no effect on PDF-induced angiogenesis. Since major differences between both PDF-dissolved AG formulations are their acidity and the bicarbonate concentration, these data suggest that this differential response is related either to pH or the presence of bicarbonate. On one hand, it has been described that alkalosis is a driving force behind Vascular endothelial growth factor (VEGF) production [19]. This might also explain the increased microvascular permeability upon AG-bicarbonate supplementation to PDF. VEGF is also involved in angiogenesis, which we, however, showed to be repressed by AG-bicarbonate. Hence, at present the relation between high pH of PDF/AG-bicarbonate, albumin leakage and repressed angiogenesis remains unclear. On the other hand, the quick capacity of the peritoneum to correct the pH of the solutions has been well recognized. Therefore, we suggest that the differential response of both formulation of AG is likely due to the protective effect of bicarbonate.

It is worth noting that AG has an inhibitory effect on not only GDPs and AGEs, but also on inducible NO

synthase [8], although we did not demonstrate that in this study. From the elegant studies of Devuyst *et al.* [3], it is known that NO is a critical determinant in the induction of functional and structural changes of the peritoneal membrane during PD and peritonitis. Beneficial effects of AG found in the present study could thus partly be explained by the ability of AG to inhibit NO synthesis. Furthermore, we cannot exclude the possibility that the reduction of PDF-induced leukocyte rolling by AG is (partly) due to a reduced NO activity. Since it is known that increased NO activity leads to reduced leukocyte rolling and adhesion [20], we believe that the AG-induced decreased rolling is most likely due to its inhibitory effects on GDPs and/or AGEs rather than on NO synthesis.

Despite the fact that AG was able to prevent various pathological changes, the oral application of high concentrations of AG was found to be toxic in diabetic patients [7]. Specifically, AG trapped pyridoxal and subsequently caused neurotoxic complications and vitamin B6 deficiency in experimental models for diabetic nephropathy [7]. In this respect, AG-pyridoxal adduct found to be superior to AG alone, as it not only prevents vitamin B6 deficiency, but is also better at controlling diabetic nephropathy [7]. Nevertheless, in PD patients, AG or related compounds, such as AG-pyridoxal adduct, could be supplemented with PDF and applied locally and in much lower concentrations than in the diabetes field. More importantly, our findings highlight the involvement of GDPs, AGEs and/or NO in the pathophysiology of PD-related complications.

Acknowledgements. This study was financially supported by the Dutch Kidney Foundation. Grant # 97.1705 and Baxter Health Care.

Conflict of interest statement. None declared.

References

1. Davies SJ, Phillips L, Naish PF, Russell GI. Peritoneal glucose exposure and changes in membrane solute transport with time on peritoneal dialysis. *J Am Soc Nephrol* 2001; 12: 1046–1051
2. Schalkwijk CG, Posthuma N, ten Brink HJ *et al*. Induction of 1,2-dicarbonyl compounds, intermediates in the formation of advanced glycation end-products, during heat-sterilization of glucose-based peritoneal dialysis fluids. *Perit Dial Int* 1999; 19: 325–333
3. Miyata T, Devuyst O, Kurokawa K, van Ypersele de Strihou C. Toward better dialysis compatibility: advances in the biochemistry and pathophysiology of the peritoneal membranes. *Kidney Int* 2002; 61: 375–386
4. Hekking LH, Zareie M, Driesprong BA *et al*. Better preservation of peritoneal morphologic features and defense in rats after long-term exposure to a bicarbonate/lactate-buffered solution. *J Am Soc Nephrol* 2001; 12: 2775–2786
5. Zareie M, Hekking LHP, Welten AGA-*et al*. Contribution of lactate buffer, glucose and glucose degradation end products to peritoneal injury *in vivo*. *Nephrol Dial Transplant* 2003; 18: 2629–2637
6. Miyata T, Kurokawa K, Van Ypersele De Strihou C. Advanced glycation and lipoxidation end products: role of reactive carbonyl compounds generated during carbohydrate and lipid metabolism. *J Am Soc Nephro* 2000; 11: 1744–1752
7. Miyoshi H, Taguchi T, Sugiura M *et al*. Aminoguanidine pyridoxal adduct is superior to aminoguanidine for preventing diabetic nephropathy in mice. *Horm Metab Res* 2002; 34: 371–377
8. Giri SN, Biring I, Nguyen T *et al*. Abrogation of bleomycin-induced lung fibrosis by nitric oxide synthase inhibitor, aminoguanidine in mice. *Nitric Oxide* 2002; 7: 109–118
9. Thornalley PJ. Use of aminoguanidine (Pimagedine) to prevent the formation of advanced glycation end products. *Arch Biochem Biophy* 2003; 419: 31–40
10. Lamb EJ, Cattell WR, Dawnay AB. *In vitro* formation of advanced glycation end products in peritoneal dialysis fluid. *Kidney Int* 1995; 47: 1768–1774
11. Lee EA, Oh JH, Lee HA *et al*. Structural and functional alterations of the peritoneum after prolonged exposure to dialysis solutions: role of aminoguanidine. *Perit Dial Int* 2001; 21: 245–253
12. Rashid G, Luzon AA, Korzets Z *et al*. The effect of advanced glycation end-products and aminoguanidine on TNFalpha production by rat peritoneal macrophages. *Perit Dial Int* 2001; 21: 122–129
13. Zareie M, van Lambalgen AA, De Vriese AS *et al*. Increased leukocyte rolling in newly formed mesenteric vessels in the rat during peritoneal dialysis. *Perit Dial Int* 2002; 22: 655–662
14. Bobbink IW, de Boer HC, Tekelenburg WL *et al*. Effect of extracellular matrix glycation on endothelial cell adhesion and spreading: involvement of vitronectin. *Diabetes* 1997; 46: 87–93
15. Mortier S, De Vriese AS, McLoughlin RM *et al*. Effects of conventional and new peritoneal dialysis fluids on leukocyte recruitment in the rat peritoneal membrane. *J Am Soc Nephrol* 2003; 14: 1296–1306
16. Malyszko J, Malyszko JS, Mysliwiec M. Endothelial cell injury markers in chronic renal failure on conservative treatment and continuous ambulatory peritoneal dialysis. *Kidney Blood Press Res* 2004; 27: 71–77
17. Welten AG, Schalkwijk CG, ter Wee PM *et al*. Single exposure of mesothelial cells to glucose degradation products (GDPs) yields early advanced glycation end-products (AGEs) and a proinflammatory response. *Perit Dial Int* 2003; 23: 213–221
18. Mortier S, Faict D, Schalkwijk CG, Lameire NH, De Vriese AS. Long-term exposure to new peritoneal dialysis solutions: effects on the peritoneal membrane. *Kidney Int* 2004; 66: 1257–1265
19. Brooks SE, Gu X, Kaufmann PM *et al*. Modulation of VEGF production by pH and glucose in retinal Muller cells. *Curr Eye Res* 1998; 17: 875–882
20. Benjamim CF, Silva JS, Fortes ZB *et al*. Inhibition of leukocyte rolling by nitric oxide during sepsis leads to reduced migration of active microbicidal neutrophils. *Infect Immun* 2002; 70: 3602–3610

Received for publication: 11.5.05
Accepted in revised form: 12.8.05